Structure of Al(100)-$c(2\times2)$-Li: A binary surface alloy

J. H. Petersen, A. Mikkelsen, M. M. Nielsen, and D. L. Adams
Institute of Physics and Astronomy, Aarhus University, DK-8000 Aarhus C, Denmark
(Received 22 March 1999)

The atomic geometry of the Al(100)-$c(2\times2)$-Li phase formed by adsorption of $\frac{1}{2}$-ML Li on Al(100) at room temperature has been determined by analysis of extensive low energy electron-diffraction (LEED) measurements. The structure is found to be a binary surface alloy, in which Li atoms occupy fourfold-coordinated substitutional sites formed by displacing every second Al atom in the first layer of the substrate. The surface structure is very similar to the (100) plane of the metastable, bulk Al_3Li alloy. An analysis of experimental LEED data for clean Al(100) leads to the conclusions that the first interlayer spacing is expanded by about 2% with respect to the bulk value, and that the vibrations of Al atoms in the first layer are about twice as large as for atoms in the bulk. Adsorption of Li leads to a contraction of nearly 6% of the first Al-Al interlayer spacing, and further enhances the vibrations of Al atoms in the first, mixed Al/Li layer [S0163-1829(99)16331-8]

I. INTRODUCTION

Following the discovery,[1] by analysis of surface extended x-ray absorption fine-structure measurements, that the adsorption of Na at room temperature on Al(111) leads to a reconstruction of the substrate, subsequent low-energy electron diffraction[2–9] (LEED) and core-level spectroscopy[10–14] studies have shown that surface reconstruction is a general consequence of the adsorption of alkali metals on Al surfaces at room temperature. Thus adsorption of Li, Na, K, Rb, and Cs on Al(111) leads to the formation of binary surface alloys, and coadsorption of Na with K, Rb, or Cs leads to the formation of ternary surface alloys. These results were particularly unexpected in that Na, K, Rb, and Cs are immiscible[15] in Al. The study of Li adsorption on Al surfaces is of special interest in that Li *is* miscible in Al, with which it forms a stable, bulk AlLi alloy with a bcc-like NaTl structure, and a metastable Al_3Li alloy with a fcc-like Cu_3Au structure[16]. Thus studies of the adsorption of Li on Al surfaces can conceivably give insight into the initial stages of alloy formation. In a previous study[7] of Li adsorption on Al(111), we have shown that Li atoms occupy sixfold substitutional sites in the Al(111)-$(\sqrt{3}\times\sqrt{3})R30°$ phase formed by adsorption of $\frac{1}{3}$ ML Li at room temperature. In the present study it is shown that the Al(100)-$c(2\times2)$-Li phase formed by adsorption of $\frac{1}{2}$-ML Li at room temperature contains Li atoms in fourfold substitutional sites, similar to the corresponding Al(100)-$c(2\times2)$-Na phase.[17] The structure is very similar to the (100) plane of the metastable Al_3Li bulk alloy.

In the following, the experimental procedures used in this study are described in Sec. II. The procedures used in the calculation of LEED intensities and in analysing the data are described in Secs. III and IV, respectively. The results of the data analysis are presented in Sec. V, and discussed in Sec. VI.

II. EXPERIMENTAL PROCEDURES

The measurements were carried out in a new experimental system consisting of a Vacuum Generators (VG) μ-metal ultra-high vacuum chamber, fitted with an Omicron reverse-view LEED optics, a VG AX100 electron spectrometer and LEG61 electron gun for Auger electron spectroscopy (AES), a VG EX05 sputter gun for sample cleaning, a VG Quartz quadrupole mass spectrometer, and a VG HPT manipulator.

LEED intensity measurements were made using a newly developed digital LEED system,[18] in which the LEED pattern on the fluorescent screen of the reverse-view LEED optics is recorded using a Princeton slow-scan CCD camera with a Nikkor 28-mm $f/2.0$ lens. The camera is based on a SITe back-illuminated CCD chip with a geometric resolution of 512×512 pixels and with an intensity resolution of 16 bits. The CCD chip is Peltier cooled to $-40\,°C$. The electron-beam energy is programmed and read using a National Instruments 16 bit a/d converter, which is also used to read the incident electron-beam current. The measurements are carried out under computer control using a PC with 200-MHz Intel Pentium Pro CPU running the Windows 95 operating system.

A complete set of typically 400 images of the LEED pattern as a function of the incident electron energy can be recorded and saved in about 20 min using the 16-bit mode of the camera controller. Because of the large dynamic range and low noise of the camera system, a single set of images at fixed optical gain is sufficient to enable accurate measurements to be made of the intensities of all the diffracted beams. A corresponding set of measurements using the 12-bit mode of the camera controller can be carried out in about 5 min. Such measurements are useful for setup purposes, including alignment of the crystal by comparison of measurements of (nominally) symmetry-equivalent beams. The final intensities are obtained in an accurate, off-line analysis of stored 16-bit images, which involves a parametrization of the background and spot profiles. The intensities are normalized for the variation of the incident-beam current with energy and for the Lambert's law dependence of the spot intensity with position on the fluorescent screen.

The Al(100) crystal could be cooled to 100 K using liquid nitrogen and heated by electron bombardment. The crystal was cleaned by cycles of Ar^+ bombardment and annealing to 750 K. Lithium was deposited onto the crystal by evaporation from an SAES source. The deposition was carried out in a few minutes and the residual-gas pressure during evapora-

TABLE I. Best-fit parameter values for clean Al(100) and for Li adsorbed in the substitutional site in the Al(100)-$c(2\times2)$-Li structure. The interlayer spacings are denoted d_j and the rms vibrational amplitudes are denoted u_j, where the subscripts indicate the layers in question. Δr_3 is the rumpling of Al atoms in the third layer (see text). For the $c(2\times2)$-Li phase, results are shown of the analyses of measurements at $\theta = 0°$ and 8.9°. The final column gives the weighted means of the results of these two analyses.

	1×1	$c(2\times2)$-Li		
θ	0°	0°	8.9°	weighted mean
$d_{Li\text{-}Al_1}$		0.35±0.05 Å	0.28±0.05 Å	0.32±0.04 Å
$d_{Al_1\text{-}Al_2}$	2.06±0.02 Å	1.89±0.03 Å	1.92±0.05 Å	1.90±0.03 Å
Δr_3		0.03±0.02 Å	0.03±0.02 Å	0.03±0.01 Å
$d_{Al_2\text{-}Al_3}$	2.04±0.02 Å	2.02±0.03 Å	2.01±0.04 Å	2.02±0.02 Å
$d_{Al_3\text{-}Al_4}$	2.01±0.02 Å	2.02±0.03 Å	2.04±0.03 Å	2.03±0.02 Å
u_{Li}		0.23±0.09 Å	0.24±0.08 Å	0.24±0.06 Å
u_{Al_1}	0.17±0.02 Å	0.21±0.02 Å	0.27±0.02 Å	0.24±0.01 Å
u_{Al_2}	0.14±0.02 Å	0.14±0.03 Å	0.19±0.03 Å	0.17±0.02 Å
u_{Al_3}	0.10±0.02 Å	0.12±0.03 Å	0.14±0.03 Å	0.13±0.02 Å
$u_{Al_{bulk}}$	0.08±0.02 Å	0.11±0.02 Å	0.09±0.02 Å	0.10±0.01 Å
V_{im}	5.1±0.8 eV	3.1±0.7 eV	5.3±0.8 eV	4.1±0.5 eV
R	0.021	0.055	0.073	

tion was typically 2×10^{-10} torr. AES measurements taken after deposition and after completion of a set of LEED measurements indicated that surface contamination (almost entirely C) was less than 0.03 ML. The absence of significant surface contamination was also indicated by the fact that consecutive measurements of LEED intensity-energy spectra for the $c(2\times2)$-Li phase recorded with an interval of 1 h showed essentially no changes. Sharp $c(2\times2)$ LEED patterns with good contrast were obtained after deposition of $\frac{1}{2}$-ML Li at 300 K. Further deposition of Li led to a decrease in intensity of the fractional-order beams, but no new ordered structures were observed. The optimum development of the $c(2\times2)$ structure was achieved by incremental deposition of Li until a maximum was reached in the ratio of integrated intensity in fractional- and integral-order diffracted beams. After each adsorption experiment, Li was removed by Ar^+ bombardment, rather than by thermal desorption, to minimize possible diffusion of Li into the bulk of the crystal. With this procedure, no evidence of such diffusion was observed in the course of many experiments.

Core-level spectroscopy measurements using synchrotron radiation, carried out using a Scienta electron spectrometer in a separate vacuum system on a spherical grating monochromator (SGM) beam line at the storage ring ASTRID in Århus, indicated that adsorption of Li below $\frac{1}{2}$ ML gives rise to a single adsorbed state with a Li 1s binding energy of 55.60 eV. Adsorption beyond $\frac{1}{2}$ ML leads to the formation of a second adsorbed state with a 1s binding energy of 54.60 eV, attributed to the growth of a Li underlayer.[19]

Intensity-energy spectra were measured for the clean Al(100) surface at 100 K and for the $c(2\times2)$-Li phase at 100 K after adsorption of Li at 300 K, in the energy range 50–450 eV with a step size of 1 eV. Measurements for the clean surface were made at normal incidence $\theta=0°$. Measurements for the $c(2\times2)$-Li phase were made both at normal incidence and at $\theta=8.9°$. The measurements at $\theta=8.9°$ were made with an azimuthal angle $\phi=0°$, in order

TABLE II. Comparison of the present results for Al(100)-(1×1) and Al(100)-$c(2\times2)$-Li with the results of Berndt *et al.* (Ref. 17) for Al(100)-(1×1) and Al(100)-$c(2\times2)$-Na. It is noted that the uncertainties given in Ref. 17 are stated to correspond to a 1% increase in the value of the R factor used there, whereas our uncertainties are estimated from a 10% increase in our R factor. The cited vibrations for the $c(2\times2)$-Na structure at 100 K have been derived from the Debye temperatures given in Ref. 17.

Reference	Present	Ref. 17	Present	Ref. 17
	1×1	1×1	$c(2\times2)$-Li	$c(2\times2)$-Na
$d_{alkali\text{-}Al_1}$			0.32±0.04 Å	1.10±0.03 Å
$d_{Al_1\text{-}Al_2}$	2.06±0.02 Å	2.08±0.004 Å	1.90±0.03 Å	1.84±0.01 Å
$d_{Al_2\text{-}Al_3}$	2.04±0.02 Å	2.01±0.008 Å	2.02±0.02 Å	2.04±0.01Å
Δr_3			0.03±0.01 Å	0.05±0.02 Å
u_{alkali}			0.24±0.06 Å	0.40±0.06 Å
u_{Al_1}	0.17±0.02 Å	0.16±0.007 Å	0.24±0.01 Å	0.22±0.02 Å
u_{Al_2}	0.14±0.02 Å	0.12±0.005 Å	0.17±0.02 Å	0.15±0.01 Å
u_{Al_3}	0.10±0.02 Å	0.09±0.005 Å	0.13±0.02 Å	
$u_{Al_{bulk}}$	0.08±0.02 Å		0.10±0.01 Å	

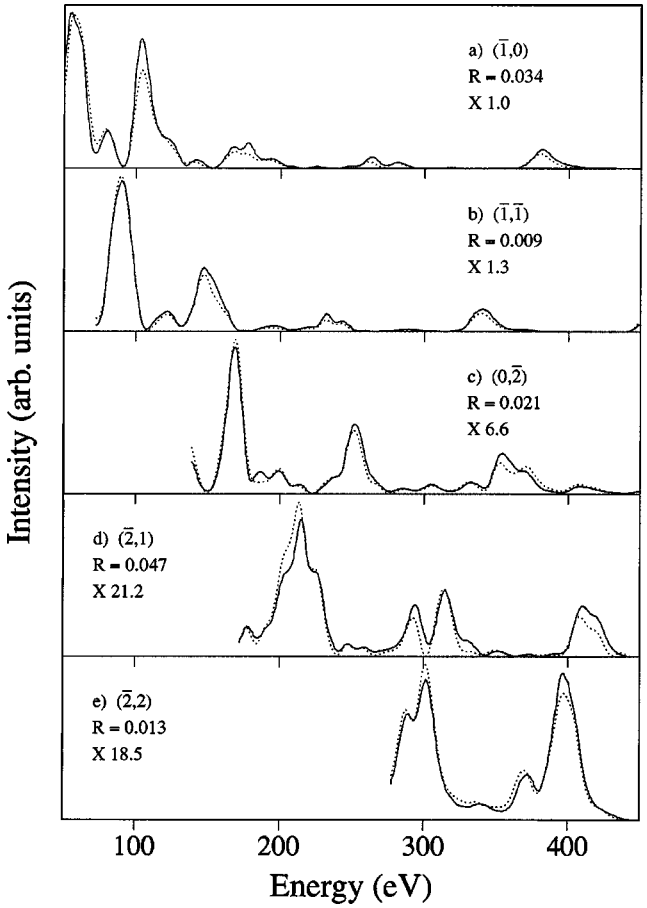

FIG. 1. (a)–(e) Comparison of experimental (solid lines) and calculated (dotted lines) intensity-energy spectra for clean Al(100) at $\theta=0°$ for five integral-order beams. The beam hk indices, R factors, and scale factors are shown in each panel. The calculated spectra were obtained using the best-fit parameter values given in Table I.

to preserve mirror-plane symmetry. For the clean surface, intensity-energy spectra were measured for a total of 33 diffracted beams, reducing to seven symmetry-inequivalent beams after averaging over symmetry-equivalent beams. For the $c(2\times2)$-Li phase, measurements were made for a total of 60 diffracted beams at $\theta=0°$, reducing to seven integral-order and five fractional-order symmetry-inequivalent beams. At $\theta=8.9°$ measurements were made for a total of 49 diffracted beams, reducing to 20 integral-order and ten fractional-order symmetry-inequivalent beams. In each set of measurements, the intensities of *all* diffracted beams contained in the solid angle defined by the LEED optics were measured, except for a few beams whose trajectories were blocked by the electron gun and/or its connections, and beams for which the accessible energy range was less than about 30 eV.

III. LEED INTENSITY CALCULATIONS

LEED intensities were calculated using the dynamical theory of LEED, with computer programs derived originally[20] from the layer-doubling and combined-space programs of Pendry[21] and Van Hove and Tong.[22] Atomic scattering matrices for Al and Li were calculated using phase

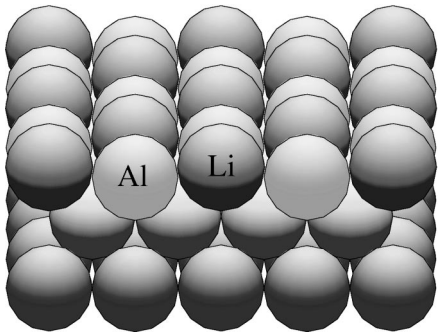

FIG. 2. Hard-sphere model of the geometry of the Al(100)-$c(2\times2)$-Li structure, shown as a central projection on the (211) plane, tilted by 20° with respect to the plane of the paper.

shifts calculated from the muffin-tin band-structure potentials of Moruzzi *et al.*,[23] and were renormalized for the effects of thermal vibrations using root-mean-square (rms) isotropic vibrational amplitudes u_{Li} for the adsorbed Li atoms, u_{Al_1}, u_{Al_2}, and u_{Al_3} for Al atoms in the first, second, and third Al layers, and $u_{Al_{bulk}}$ for the Al substrate. Up to 196 partial waves (14 phase shifts) and 193 plane waves (reduced by symmetry to 31, and 101 symmetry-adapted plane waves at $\theta=0°$ and 8.9°, respectively) were used in the L space and k-space treatments, respectively, of multiple scattering within and between layers parallel to the surface.

The complex electron self-energy $\Sigma=V_0+iV_{im}$ was taken to be independent of energy. The surface potential barrier was taken to be a refracting but nonreflecting step of height V_0, positioned at a distance equal to one-half the bulk interlayer spacing above the first layer of atoms. We estimate that the calculations are a numerically accurate reflection of the model assumptions to better than 2%. All calculations used in the structure determination were carried out with full accuracy.

IV. SURFACE STRUCTURE DETERMINATION

A preliminary survey of structural models compatible with the observed symmetry of the diffracted intensities, involving Li adsorbed in on-top, fourfold hollow, and fourfold substitutional sites, indicated clearly that only the latter model warranted further refinement. A full optimization of the fit between experimental intensities and intensities calculated for Li adsorbed in the substitutional site was then carried out using a semiautomatic implementation of an iterative procedure described previously,[7,20] in which the disagreement between experimental and calculated intensities, as measured by an R factor, is minimized as a function of one variable at a time. The procedure contains an inner loop in which the structural variables are optimized iteratively, and an outer loop in which the nonstructural variables are optimized iteratively. The inner loop is executed automatically in a single computer run, but the outer loop is currently executed manually. The procedure is very efficient by virtue of maximum reuse of intermediate calculations.

The calculational variables in the present work comprised the interlayer spacings $d_{Li\text{-}Al_1}$, $d_{Al_1\text{-}Al_2}$, $d_{Al_2\text{-}Al_3}$, and $d_{Al_3\text{-}Al_4}$;

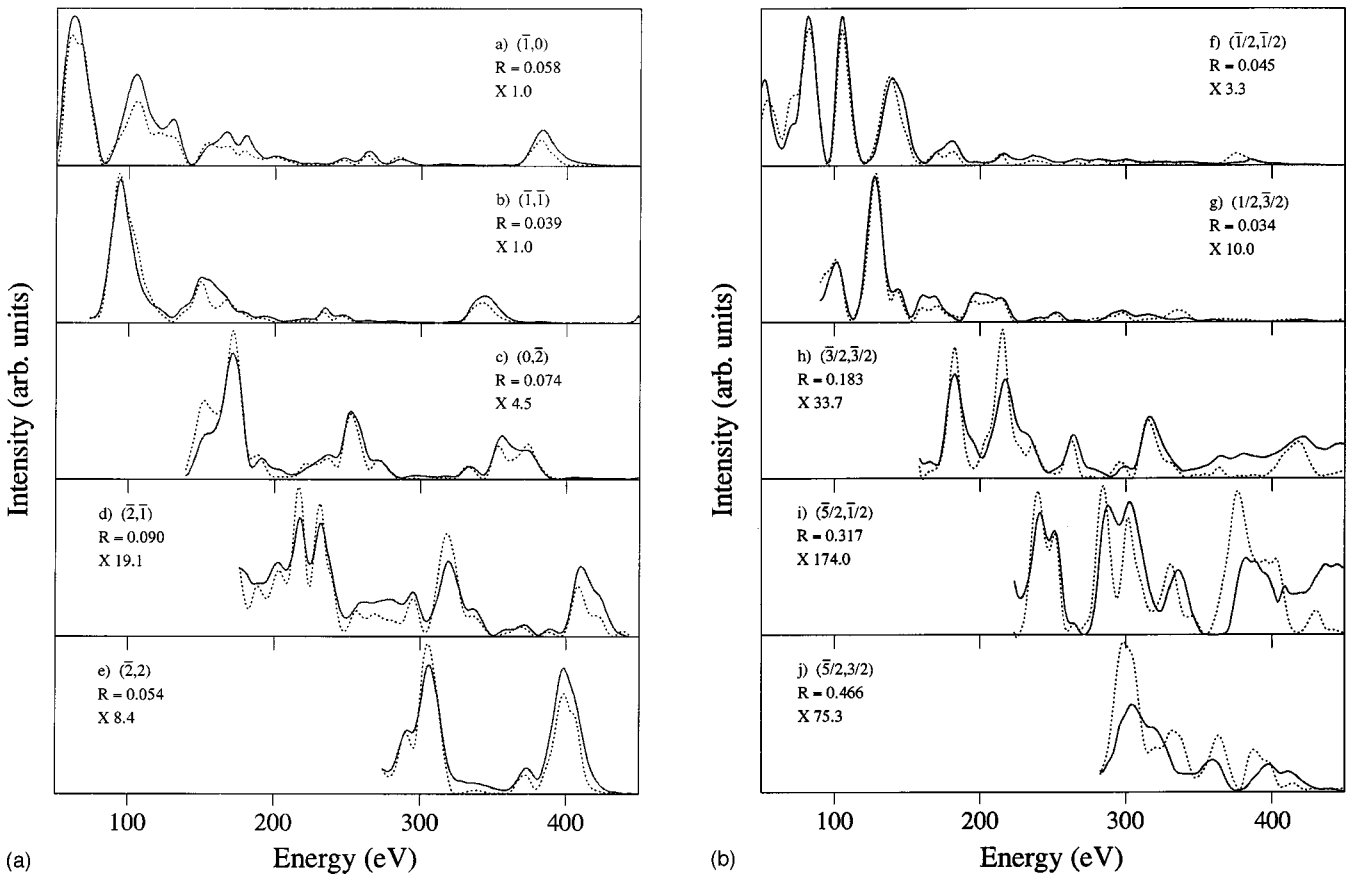

FIG. 3. Comparison of experimental (solid lines) and calculated (dotted lines) intensity-energy spectra for Al(100)-$c(2\times2)$-Li at $\theta=0°$ for five integral-order beams [(a)–(e)], and five fractional-order beams [(f)–(j)]. The beam hk indices, R factors, and scale factors are shown in each panel. The calculated spectra were obtained using the best-fit parameter values given in Table I.

a vertical displacement toward the surface Δr_3 of those atoms in the third Al layer that lie beneath adsorbed Li atoms; the vibrational amplitudes u_{Li}, u_{Al_1}, u_{Al_2}, u_{Al_3}, and $u_{Al_{bulk}}$; and the real and imaginary parts of the electron self-energy V_0 and V_{im}, respectively.

The R factor is a normalized χ^2 function defined[5,7,24] as

$$R=\sum_{hk,i}\left(\frac{I^{ex}_{hk,i}-cI^{cal}_{hk,i}}{\sigma_{hk}}\right)^2\Bigg/\sum_{hk,i}\left(\frac{I^{ex}_{hk,i}}{\sigma_{hk}}\right)^2, \tag{1}$$

where c is a *global* scaling constant between the experimental $I^{ex}_{hk}(E)$ and calculated intensities $I^{cal}_{hk}(E)$, and σ_{hk} is the root-mean-square experimental uncertainty of the beam hk, obtained[7] via comparison of measurements for (nominally) symmetry-equivalent beams. The scaling constant c is determined by the requirement that $\partial R/\partial c=0$ as

$$c=\sum_{hk,i}\left(\frac{I^{ex}_{hk,i}I^{cal}_{hk,i}}{\sigma^2_{hk}}\right)\Bigg/\sum_{hk,i}\left(\frac{I^{cal}_{hk,i}}{\sigma_{hk}}\right)^2. \tag{2}$$

Substitution for c in Eq. (1) leads to

$$R=1-\left[\sum_{hk,i}\left(\frac{I^{ex}_{hk,i}I^{cal}_{hk,i}}{\sigma_{hk}}\right)\right]^2\Bigg/\sum_{hk,i}\left(\frac{I^{ex}_{hk,i}}{\sigma_{hk}}\right)^2\sum_{hk,i}\left(\frac{I^{cal}_{hk,i}}{\sigma_{hk}}\right)^2, \tag{3}$$

from which it follows that R is bounded by 0 and 1.

V. RESULTS

The results of structural analyses for clean Al(100), and for Al(100)-$c(2\times2)$-Li with Li adsorbed in the substitutional site, are listed in Table I.

A. Al(100)-(1×1)

The structure of clean Al(100) is shown to involve small expansions of the first and second interlayer spacings of $2.0\pm0.8\%$ and $1.2\pm0.7\%$, respectively. As can be seen from the results in Table I, the vibrations of Al atoms in the first layer are twice as large as for Al atoms in the bulk. The enhanced surface vibrations decay to the bulk value within the first four layers. Except for the expansion of the second interlayer spacing, these results are in agreement to within estimated uncertainties with the results of a recent study by Berndt *et al.*,[17] as shown in Table II and discussed below. A plot of experimental intensity spectra and spectra calculated for the optimum parameter values given in Table I is shown in Fig. 1.

B. Al(100)-$c(2\times2)$-Li

Separate, full optimizations were carried out for the data sets at $\theta=0°$ and 8.9°, respectively. As can be seen from Table I, the parameter values determined from the two separate optimizations agree to within the estimated uncertainties. We note, however, that the uncertainties in the Li-Al

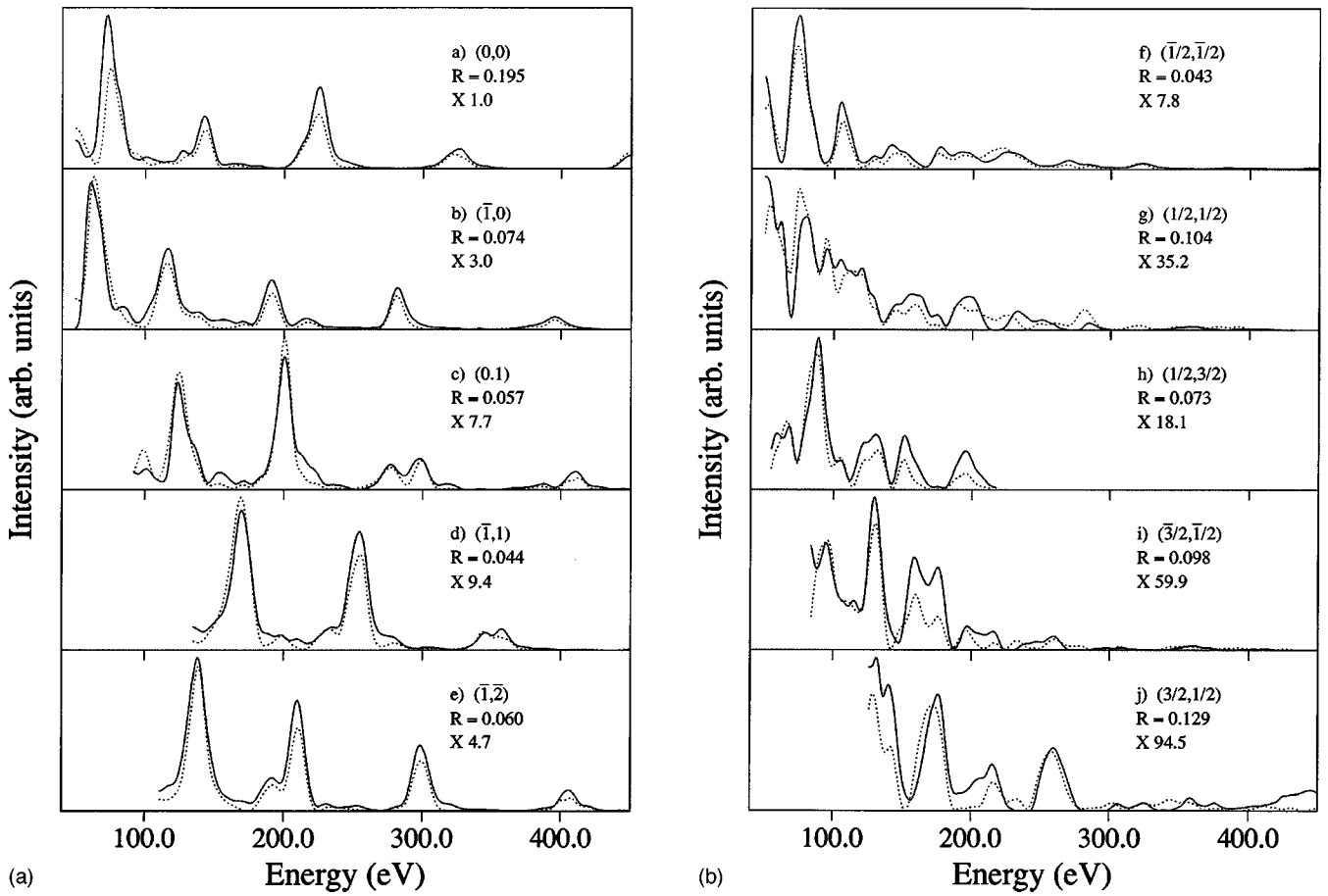

FIG. 4. Comparison of experimental (solid lines) and calculated (dotted lines) intensity-energy spectra for Al(100)-$c(2\times2)$-Li at $\theta = 8.9°$ for five integral-order beams [(a)–(e)], and five fractional-order beams [(f)–(j)]. The beam hk indices, R factors, and scale factors are shown in each panel. The calculated spectra were obtained using the best-fit parameter values given in Table I.

layer spacing and in the vibrational amplitudes of adsorbed Li are large. As in the case of the Al(111)-($\sqrt{3}\times\sqrt{3}$)$R30°$-Li structure,[7] the large uncertainties can probably be attributed to the relatively weak scattering from Li atoms.

It is interesting to note that the vertical spacing between Al atoms in the first, mixed Al/Li layer and Al atoms in the second layer corresponds to a $-5.8\pm1.5\%$ contraction with respect to the bulk interlayer spacing, as can be compared to the $2.0\pm0.8\%$ expansion of the first interlayer spacing in the clean Al(100) surface. We also note that the substitutional adsorption of Li in the first Al layer induces a small ($\Delta r_3 = 0.03$Å) rumpling of the third Al layer, such that the Al atoms in this layer which are directly beneath Li atoms in the first mixed Al/Li layer are displaced toward the surface. Finally, we note that the vibrational amplitudes of Al atoms in the first, mixed Al/Li layer are even larger than is the case for the clean Al(100) surface.

A hard-sphere model of the Al(100)-$c(2\times2)$-Li structure is shown in Fig. 2. Plots of experimental intensity spectra and spectra calculated for the optimum parameter values given in Table I are shown in Figs. 3 and 4 for $\theta=0°$ and 8.9°, respectively. We note that the plots have been constructed using a single, beam-independent, scaling factor between experiment and calculations [Eq. (2)]. We regard the overall level of agreement between experiment and theory as satisfactory, although less definitive than in our previous analyses[9] of the surface structures formed by the heavier alkalis. The residual discrepancies between experiment and theory, and the generally larger R factors for the fractional-order beams, are perhaps due to a less than perfect order in the $c(2\times2)$-Li structure.

VI. SUMMARY AND DISCUSSION

In summary, the present work has shown that the Al(100)-$c(2\times2)$-Li phase formed by adsorption of $\frac{1}{2}$-ML Li on Al(100) at room temperature consists of a binary surface alloy. Li atoms occupy substitutional sites formed by displacement of $\frac{1}{2}$-ML Al atoms from the first layer of the substrate. The spacing between the Li layer and the reconstructed Al layer is 0.32 ± 0.04 Å, and the rms isotropic vibrational amplitude of adsorbed Li atoms is 0.24 ± 0.06 Å. The corresponding hard-sphere radius of the Li atoms is 1.44 Å , as compared to the bulk (bcc) metallic radius[25] of 1.52 Å. The Li-Al bond length is 2.87 Å.

In addition to the reconstruction of the first Al layer, the adsorption of Li results in strong perturbations to the properties of the substrate. Thus the expansion of 2.0% of the first interlayer spacing in the clean Al(100) surface is transformed to a contraction of 5.8% in the $c(2\times2)$-Li phase. Furthermore, the enhanced vibrational amplitudes found for Al atoms in the first layer of the clean substrate are even larger after adsorption of Li.

The results reported here are very similar to those re-

ported by Berndt *et al.*[17] for Al(100)-(1×1) and Al(100)-$c(2\times2)$-Na, as can be seen from the comparison given in Table II. First, we note that the interlayer spacings and vibrations determined here for the clean Al(100) surface are in good agreement with those determined previously, except for the value of the second interlayer spacing where we find a small expansion. The small differences between the two determinations can perhaps be attributed to the greater accuracy of the present calculations which used 14 phase shifts as compared to the nine phase shifts used in the previous study. As far as the $c(2\times2)$-Li and $c(2\times2)$-Na structures are concerned, it can be seen that these are very similar, except of course for the shorter Al-Li bond distance. As found here for Li, strong perturbations of the substrate result from the adsorption of Na, including a contraction of the first Al-Al interlayer spacing and a further enhancement of the vibrational amplitudes of Al atoms in the first two layers. Finally, we note that the surface structure of the Al(100)-$c(2\times2)$-Li phase, as determined here, is very similar to that of the (100) plane of the metastable Al_3Li bulk alloy.

ACKNOWLEDGMENTS

Support of this work by the Danish Natural Science Research Council is gratefully acknowledged.

[1] A. Schmalz, S. Aminpirooz, L. Becker, J. Haase, J. Neuegebauer, M. Scheffler, D. R. Batchelor, D. L. Adams, and E. Bøgh, Phys. Rev. Lett. **67**, 2163 (1991).
[2] C. Stampfl, M. Scheffler, H. Over, J. Burchhardt, M. M. Nielsen, D. L. Adams, and W. Moritz, Phys. Rev. Lett. **69**, 1532 (1992).
[3] C. Stampfl, M. Scheffler, H. Over, J. Burchhardt, M. M. Nielsen, D. L. Adams, and W. Moritz, Phys. Rev. B **49**, 4959 (1992).
[4] M. M. Nielsen, J. Burchhardt, D. L. Adams, E. Lundgren, and J. N. Andersen, Phys. Rev. Lett. **72**, 3370 (1994).
[5] J. Burchhardt, M. M. Nielsen, D. L. Adams, E. Lundgren, and J. N. Andersen, Phys. Rev. B **50**, 4718 (1994).
[6] J. Burchhardt, M. M. Nielsen, D. L. Adams, E. Lundgren, J. N. Andersen, C Stampfl, M. Scheffler, A. Schmalz, S. Aminpirooz, and J. Haase, Phys. Rev. Lett. **74**, 1617 (1995).
[7] M. M. Nielsen, S. V. Christensen, and D. L. Adams, Phys. Rev. B **54**, 17 902 (1996).
[8] S. V. Christensen, J. Nerlov, K. Nielsen, J. Burchhardt, M. M. Nielsen, and D. L. Adams, Phys. Rev. Lett. **76**, 1892 (1996).
[9] D. L. Adams, Appl. Phys. **62**, 123 (1996), and references therein.
[10] J. N. Andersen, M. Quarford, R. Nyholm, J. J. van Acker, and E. Lundgren, Phys. Rev. Lett. **68**, 94 (1992).
[11] J. N. Andersen, E. Lundgren, R. Nyholm, and M. Quarford, Phys. Rev. B **46**, 12 784 (1992).
[12] J. N. Andersen, E. Lundgren, R. Nyholm, and M. Quarford, Surf. Sci. **289**, 307 (1993).
[13] E. Lundgren, R. Nyholm, J. Burchhardt, D. Heskett, and J. N. Andersen, Surf. Sci. **343**, 37 (1995).
[14] J. N. Andersen, Surf. Rev. Lett. **2**, 345 (1995), and references therein.
[15] *Pearson's Handbook of Crystallographic Data for Intermetallic Phases* (ASM International, Materials Park, OH, 1991).
[16] W. B. Pearson, *The Crystal Chemistry and Physics of Metals and Alloys* (Wiley, New York, 1972).
[17] W. Berndt, D. Weick, C. Stampfl, A. M. Bradshaw, and M. Scheffler, Surf. Sci. **330**, 182 (1995).
[18] A. Mikkelsen and D. L. Adams, Phys. Rev. B **60**, 2040 (1999).
[19] J. H. Petersen, C. Søndergaard, S. V. Hoffmann, A. Mikkelsen, and D. L. Adams, Surf. Sci. (to be published).
[20] D. L. Adams, V. Jensen, X. F. Sun, and J. H. Vollesen, Phys. Rev. B **38**, 7913 (1988).
[21] J. B. Pendry, *Low Energy Electron Diffraction* (Academic Press, London, 1974).
[22] M. A. V. Hove and S. Y. Tong, *Surface Crystallography by LEED* (Springer-Verlag, Berlin, 1979).
[23] V. L. Moruzzi, J. F. Janak, and A. R. Williams, *Calculated Electronic Properties of Metals* (Pergamon, New York, 1978).
[24] M. M. Nielsen, J. Burchhardt, and D. L. Adams, Phys. Rev. B **50**, 7851 (1994).
[25] A. Taylor and B. J. Kagle, *Crystallographic Data on Metal and Alloy Structures* (Dover, New York, 1963).